International Journal of Engineering and Advanced Technology (IJEAT)
ISSN: 2249-8958 (Online), Volume-9 Issue-1, October, 2019

# Adsorption of Amido Black 10B by $ZnFe_2O_4$-ZnO Nanopowder

**M. N. Zulfiqar Ahmed, A. A. Jahagirdar, H. M. Somashekar**

***Abstract:*** ***$ZnFe_2O_4$-ZnO nanopowder was synthesized by solution combustion method using zinc nitrate and ferric nitrate as oxidizers and oxalyl dihydrazide as fuel. The nanopowder was characterized by powder X-ray diffraction (PXRD), Fourier transform infrared spectroscopy (FTIR), scanning electron microscopy (SEM) and Brunauer-Emmett-Teller (BET) surface area measurements. The nanopowder was used as adsorbent for the removal of the dye Amido Black 10B (AB 10) from its aqueous solution. The effect of dosage of the nanopowder and contact time was studied. The results indicated that the nanopowder acted as a good adsorbent for the removal of AB 10. More than 89% removal of the dye was achieved for a catalyst dosage of 0.8g of the nanopowder per liter of the dye solution. The optimum contact time was found to be 40 minutes. Adsorption isotherms and adsorption kinetic models were applied to the adsorption data to know the mechanism and kinetics of adsorption. The adsorption data fitted well for the Langmuir adsorption isotherm and followed pseudo-second order kinetics.***

***Keywords : $ZnFe_2O_4$-ZnO, solution combustion synthesis, adsorption isotherms, Amido Black 10B.***

## I. INTRODUCTION

The major pollutants of water include heavy metals, pesticides, dyes, detergents, degreasing agents, volatile organic compounds and chlorophenols [1]. Synthetic dyes are extensively used in the textile industry and are therefore common industrial pollutants [2]. The textile industry releases huge quantities of intensely coloured effluents which are highly toxic in nature besides being resistant to destruction by biological treatment methods [3]. The dyeing process employs various types of dyes based on the type of fabric. These dyes include acidic, reactive, basic, disperse, azo, diazo, anthraquinone based and metal complex dyes [4]. Azo dyes are among the toxic and most recalcitrant classes of compounds to treat due to the presence of one or more azo groups in them which are usually attached to radicals [5].

Revised Manuscript Received on October 30, 2019.
* Correspondence Author
**M. N. ZulfiqarAhmed,** Department of Engineering, Ibri College of Technology, Ibri, Sultanate of Oman. Email: zulfi_chem@yahoo.com
**A. A. Jahagirdar,** Department of Chemistry, Dr. Ambedkar Institute of Technology, Bengaluru, India. Email: jagir22@yahoo.com
**H.M. Somashekar,** Department of Mechanical Engineering, Dr. Ambedkar Institute of Technology, Bengaluru, India. Email: dr.hmsomashekar@gmail.com



Each dye contains at least one chromophore and auxochrome which impart intense colour to it which is undesirable and disgusting in wastewater. Several conventional treatment methods such as flocculation, chemical oxidation and membrane separation employed for the removal of dyes from wastewater are not effective. Adsorption is being considered as an important process for the removal of synthetic dyes from wastewater due to its imaginable opportunity to design the chemical composition of the adsorbent surface [6]-[10]. The removal of colour from wastewater is as important as the removal of other pollutants. The decolouration of effluents from textile dyeing and finishing industries is very important due to aesthetic and environmental concerns [11]-[15].

The synthesis of nano metal oxides with high surface area for use as adsorbents in the removal of dyes from wastewaters has attracted the attention of many researchers across the globe. Several nano metal oxides such as MgO, ZnO, α-$Fe_2O_3$, $TiO_2$ etc. have been used for the removal of dyes [16]. Nanocomposites are multiphase solid materials in which the average crystallite size of at least one of the phases lies in the nanometer range. These nanocomposites usually exhibit better sorption, catalytic, optical, electrical, and other special properties [17]. In comparison to their individual components, these nanocomposites are high performance materials that exhibit unusual properties in combination and are being regarded by some researchers as the materials of the 21st century [18]. They possess high specific surface area and find potential applications in gas sensors, photocatalysis and photo-electrochemical cells [19]. The synthesis of various nanocomposites such as ZnO/$TiO_2$, ZnO/$SnO_2$, ZnO/$CO_3O_4$, $TiO_2$/$SnO_2$ etc. by various methods has been reported in literature. Some of these methods include hydrothermal, chemical bath deposition, chemical vapor deposition, sol-gel and co-precipitation. However, many of these methods suffer from various drawbacks such as long reaction time, requirement of high reaction temperature and so on [20]-[22].

Solution combustion synthesis is an important method for the synthesis of a number of nano metal oxides, ferrites and other nanomaterials. It has several advantages such as low processing time, relatively lower operating-temperature, cost effectiveness, good stoichiometric control and ultrafine particle formation with narrow size distribution [23]-[25]. In the present study, we report the synthesis of the nanocomposite $ZnFe_2O_4$-ZnO by solution combustion method. The efficiency of the nanopowder as adsorbent for the removal of the azo dye Amido Black 10B (AB 10) from its aqueous solution was studied. The data was analyzed using adsorption isotherms and adsorption kinetic models.

## II. MATERIALS AND METHODS

### A. Synthesis of the $ZnFe_2O_4$-ZnO Nanopowder

All the chemicals used were procured from M/s sd Fine Chemicals Limited, India. The fuel oxalyl dihydrazide (ODH) was prepared by the reaction between diethyl oxalate and hydrazine hydrate [26]. A 1000 ppm stock solution of AB 10 was prepared using double distilled water. The stock solution was appropriately diluted to give solution of concentration 10 ppm. All the chemicals were of analytical grade and were used without purification. Double distilled water was used throughout the experiment.

Solution combustion synthesis involves combustion reaction between the oxidizer and the fuel. In case of the $ZnFe_2O_4$-ZnO nanocomposite, zinc nitrate and ferric nitrate were used as oxidizers and ODH was used as fuel. Appropriate amounts of zinc nitrate and ferric nitrate were dissolved in minimum quantity of double distilled water taken in a cylindrical pyrex dish of approximately 300 $cm^3$ capacity. Appropriate amount of ODH was added to it and the mixture was stirred magnetically for about 10 minutes and then placed on a hot plate when the excess water was evaporated and a pasty mass was left behind. The pyrex dish was then introduced into a muffle furnace maintained at about 350°C. The reaction mixture first dehydrated, ignited at one point and then burnt instantaneously resulting in the formation of the desired nanopowder. It was then cooled to room temperature and ground well (Fig. 1).

The formation of the nanopowder can be represented by (1).

$$3Zn(NO_3)_2(aq) + 2Fe(NO_3)_3\ (aq) + 6C_2H_6N_4O_2\ (s) \rightarrow ZnFe_2O_{4(s)} + 2ZnO_{(s)} + 12CO_{2(g)} + 18H_2O_{(g)} + 18N_{2(g)} \quad (1)$$

48 moles of gases were released during the formation of one mole of the $ZnFe_2O_4$-ZnO nanopowder.

**Fig. 1. The $ZnFe_2O_4$-ZnO nanopowder.**

### B. Characterization of the Nanopowder

The PXRD data of the nanopowder was used to know its phase purity and crystal structure. The PXRD data was recorded with the help of Philips X'Pert pro X-ray diffractometer. Cu $K_\alpha$ radiation ($\lambda$ = 1.5418 Å) at 40 kV was used. The mean crystallite size of the nanopowder was estimated using (2) known as the Scherer's equation [27].

$$D = \frac{k\lambda}{\beta cos\theta} \quad (2)$$

where, $D$ is the mean crystallite size, $k$ is a constant, $\lambda$ is the wavelength of the X-rays used, $\beta$ is the full width at half maximum and $\theta$ is called the Bragg's angle.

The identification of various chemical groups present in the nanopowder was done by Fourier transform infrared spectroscopy (FTIR). The FTIR spectrum of the nanopowder was recorded using Perkin-Elmer spectrometer (spectrum 1000) with KBr as the reference.

The surface morphology of the nanopowder was determined by SEM. The SEM micrograph of the nanopowder was recorded using JEOL-2100F (Japan) scanning electron microscope.

The Brunauer-Emmet-Teller (BET) surface area of the nanopowder was determined by nitrogen adsorption using the instrument MICROMERITICS GEMINE 2375. Nitrogen gas was allowed to be adsorbed onto the nanopowder at 77 K. Prior to the analysis, the nanopowder was degassed in an evacuation chamber at a temperature of 523 K under a vacuum of $10^{-6}$ Torr for 12 hours.

### C. Batch Adsorption Studies

Amido Black 10B is an amino acid staining diazo dye used for staining total protein on transferred membrane blots. It also finds applications in criminal investigations for the detection of blood present with the latent fingerprints. It has the molecular formula $C_{22}H_{14}N_6Na_2O_9S_2$ and molecular mass equal to 616.49 $gmol^{-1}$. Chemically it is 4-Amino-5-hydroxy-3-[(4-nitrophenyl)azo]-6-(phenylazo) -2,7-Naphthalene disulfonic acid disodium salt. The dye is readily soluble in water and exhibits hazardous effects such as skin and eye irritation. It also exhibits hazardous effects on ingestion and inhalation [28]-[31]. The structure and absorption spectrum of AB 10 are shown in Fig. 2 and Fig. 3 respectively. The maximum absorption was observed at a wavelength of 618 nm.

The adsorption of AB 10 by the $ZnFe_2O_4$-ZnO nanopowder was carried out in a batch mode at room temperature. 50 $cm^3$ of the 10 ppm dye solution was transferred to a 500 $cm^3$ beaker followed by addition of appropriate amount of the nanopowder. The mixture was stirred magnetically in the dark for about 30 minutes and centrifuged at around 2500 rpm for about 10 minutes. The UV-Visible spectrum of the supernatant solution was recorded in the wavelength range of 300 to 900nm. The experiments were conducted by varying the dosage of the nanopowder from 0.1 to 1.0$gL^{-1}$.

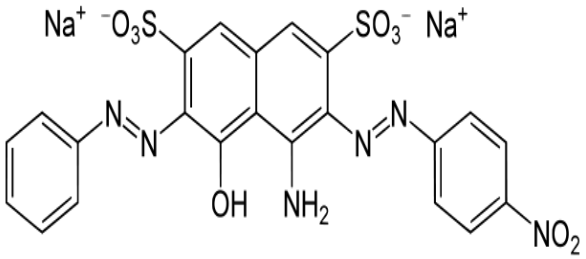


**Fig. 2. Structure of Amido Black 10B**

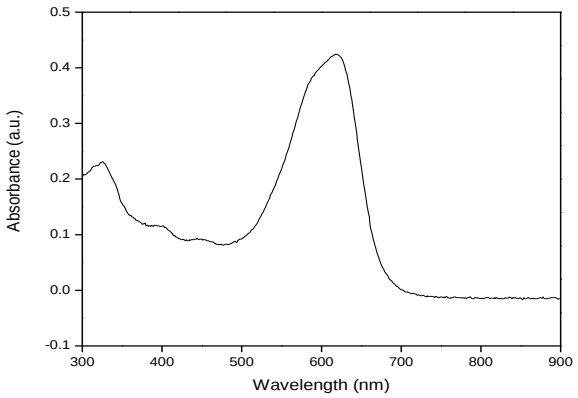


**Fig.3. Absorption spectrum of Amido Black 10B**

Equation (3) was used to calculate the percentage removal of AB 10 [32].

$$Percentage\ dye\ removal = \frac{(C_0 - C_e)\ x\ 100}{C_0} \quad (3)$$

where $C_o$ and $C_e$ represent the initial and equilibrium concentrations of the dye solution.

The optimum dosage of the nanopowder was determined by plotting the graph of $C_o/C_e$ versus the dosage of the nanopowder.

In order to determine the effect of contact time, 100 $cm^3$ of the dye solution was taken in the 500 $cm^3$ beaker and optimum amount of the nanopowder was added to it. The mixture was stirred magnetically in the dark. A small aliquot of the mixture was taken out after every 5 minutes, centrifuged and the UV-Visible spectrum was recorded as discussed earlier. The experiment was conducted upto a contact time of 120 minutes. The optimum contact time was determined by plotting the graph of $C_o/C_e$ versus the contact time.

## III. RESULTS AND DISCUSSION

### A. Characterization Results

Fig. 4 shows the PXRD pattern of the nanopowder. The diffraction peaks at (111), (220), (311), (222), (400), (422) and (511) were attributed to the spinel phase of $ZnFe_2O_4$ with a = 8.4411 A˚ (JCPDS file number: 22-1012), while the peaks at (100), (002) and (102) were attributed to the wurtzite phase of ZnO with a = 3.249A˚ and c = 5.206A˚ (JCPDS file number: 36-1451) [33]-[36]. Hence, it was concluded that the product is the coupled nanocomposite $ZnFe_2O_4$-ZnO having both zinc ferrite and zinc oxide phases. The PXRD pattern of the nanopowder exhibited high degree of crystallinity

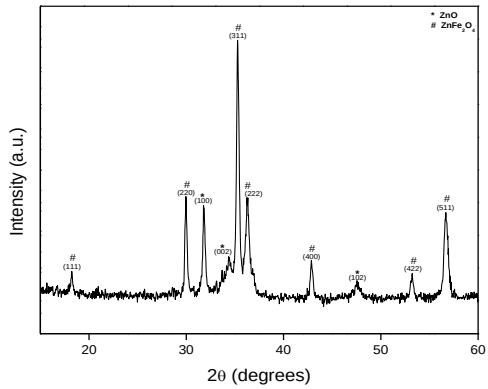


**Fig. 4. PXRD pattern of the ZnFe2O4-ZnO nanopowder**

without any impurity peak. The average crystallite size as determined by Scherer's formula was found to be around 15 nm.

Fig. 5 depicts the FTIR spectrum of the nanopowder. The peak at around 352 $cm^{-1}$ was attributed to the Zn-O bond whereas the peaks at around 416 and 542 $cm^{-1}$ were attributed to the Fe-O bond [37]-[39]. The peaks at around 2361 $cm^{-1}$ and 3434 $cm^{-1}$ were ascribed respectively to the vibrational modes of atmospheric $CO_2$ and the –OH group of water adsorbed on the surface of the nanocomposite [40]-[41].

Fig. 6 represents the SEM micrograph of the $ZnFe_2O_4$-ZnO nanopowder. The particles were agglomerated with a flake like morphology. Voids were also observed in the SEM micrograph. The presence of voids and high porosity make the nanopowder a good adsorbent material. In solution combustion synthesis, the morphological characteristics of the nanopowders are strongly dependent on the heat and gases generated during the complex decomposition. The liberation of large volumes of gases facilitates the formation of tiny particles whereas the heat released is an important factor for crystal growth. The agglomeration of the particles is usually considered as a common way of minimizing their surface free energy [42]-[43].

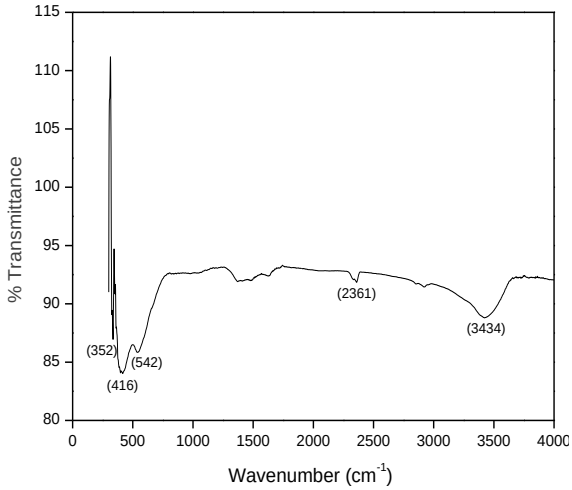


**Fig. 5. FTIR spectrum of the $ZnFe_2O_4$-ZnO nanopowder**

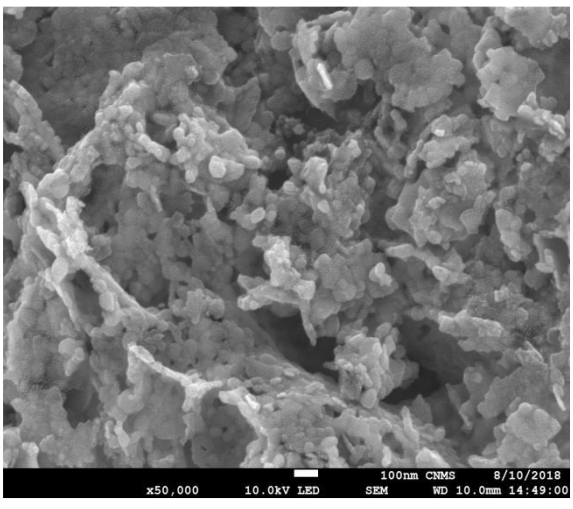


**Fig. 6. SEM micrograph of the $ZnFe_2O_4$-ZnO nanopowder**

Fig. 7 represents the plot for BET surface area of the nanopowder. The BET surface area of the nanopowder was found to be 19.22 $m^2g^{-1}$ and the mean pore diameter was found to be 4.6816 nm.

**B. Batch Adsorption Results**

Fig. 8 represents the effect of dosage of the nanopowder on the adsorption of AB 10 by the nanopowder. The amount of dye adsorbed increased with an increase in the amount of nanopowder upto an optimum dosage. This is due to the fact that an increase in the amount of nanopowder increased the number of adsorbent sites which resulted in the adsorption of more number of dye molecules on the surface. The adsorption was maximum for a catalyst dosage of 0.8 $gL^{-1}$. A further increase in the amount of the nanopowder beyond 0.8 $gL^{-1}$ resulted in negligible increase in adsorption.

Fig. 9 shows the effect of contact time on the adsorption of AB10 by the nanopowder. Maximum adsorption occurred for a contact time of 40 minutes. Beyond the optimum contact time, the dye removal was negligible. Under optimum conditions, more than 89% of the dye removal was achieved.

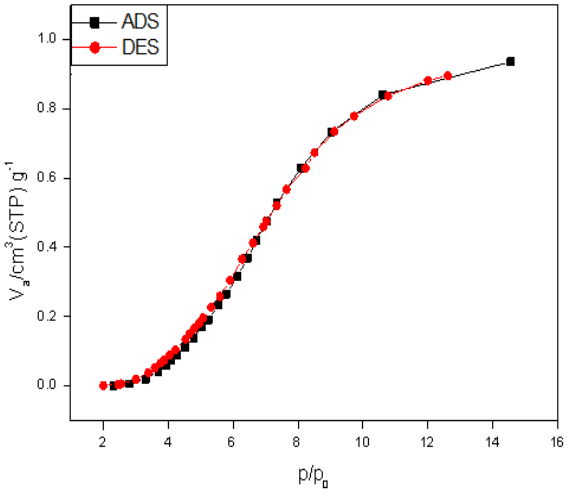


**Fig. 7. BET surface area of the ZnFe2O4-ZnO nanopowder**

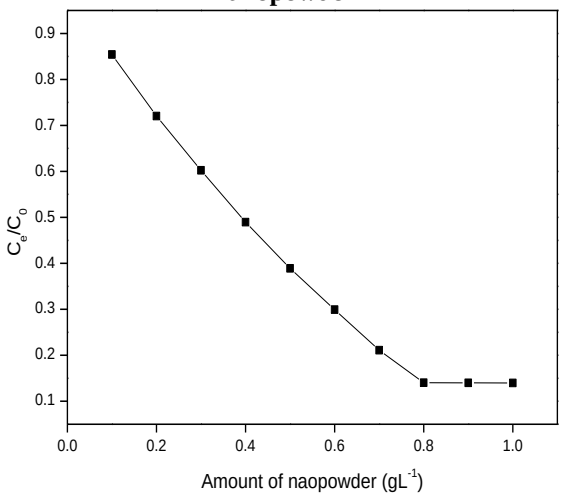


**Fig. 8. Effect of dosage of the nanopowder on the adsorption of AB 10 by the ZnFe2O4-ZnO nanopowder**

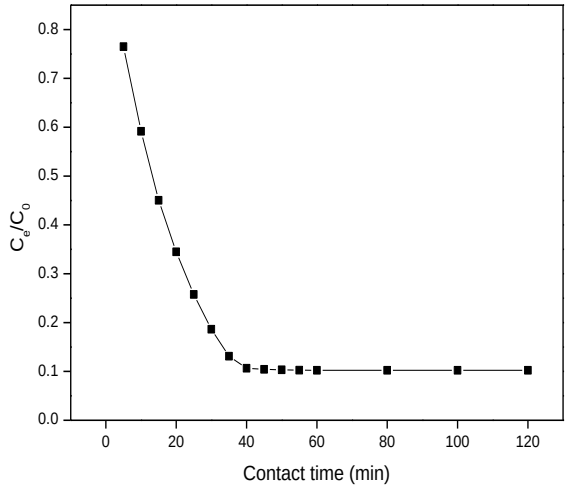


**Fig. 9. Effect of contact time on the adsorption of AB 10 by the ZnFe2O4-ZnO nanopowder**

**C. Adsorption Isotherms and Adsorption Kinetics**

The adsorption data was analyzed by Langmuir and Freundlich adsorption isotherms. The linear form of the Langmuir isotherm is given by using (4).

$$\frac{C_e}{q_e} = \frac{1}{Q_0 b} + \frac{1}{Q_0} C_e \quad (4)$$

where $q_e$ (mgg$^{-1}$) is the equilibrium adsorption capacity, $C_e$ (mgL$^{-1}$) is the equilibrium liquid phase concentration, $Q_0$ (mgg$^{-1}$) is a constant related to maximum adsorption capacity and $b$ (Lmg$^{-1}$) is the Langmuir constant related to the adsorption energy. The dimensionless constant separation factor $R_L$ was calculated using (5).

$$R_L = \frac{1}{1 + bC_0} \quad (5)$$

where $C_0$ is the initial dye concentration and $b$ has usual meaning. A value of $R_L$ between 0 and 1 indicated the feasibility of the adsorption process [44]-[45].

The Freundlich adsorption isotherm is a fairly satisfactory empirical isotherm which can be used in case of adsorption involving dilute solutions. (6) represents the linear form of the Freundlich isotherm.

$$lnq_e = lnK_F + \frac{1}{n} lnC_e \quad (6)$$

where the constant $K_F$ (mgg$^{-1}$) is related to the relative adsorption capacity; the constant $n$ (gL$^{-1}$) is related to the intensity of adsorption. A good adsorbent has a value of $n$ between 1 and 10. The lower the value of $n$, the better is the adsorption. It also indicates the formation of relatively strong bond between adsorbate and adsorbent [46].

The free energy of adsorption ($E$) was calculated by using (7).

$$E = \frac{1}{\sqrt{2K_{DR}}} \quad (7)$$

A value of $E$ between 1 and 16 kJmol$^{-1}$ indicates that the adsorption is physical in nature whereas a value of $E$ more than 16 kJmol$^{-1}$ indicates that adsorption is chemical in nature [47]. Fig. 10 and Fig. 11 represent the plots of the Langmuir and Freundlich isotherms respectively. From Table I, it is evident that the adsorption obeyed the Langmuir adsorption isotherm indicating multilayer adsorption. The value of $R_L$ was between 0 and 1 which also indicated that adsorption is a favorable process in the removal of AB 10 by the nanopowder.

The value of *E* below 16 kJmol$^{-1}$ indicated that the adsorption was mainly physical in nature.

Several mathematical models have been reported in the literature which quantitatively describe the kinetics of the adsorption process. The pseudo-first order and the pseudo-second-order models were applied to determine the kinetics of the adsorption process.

In case of pseudo-first order model, the rate constant is determined by using (8) known as the Lagergren equation [48].

$$\frac{dq_t}{dt} = k_1(q_e - q_t) \qquad (8)$$

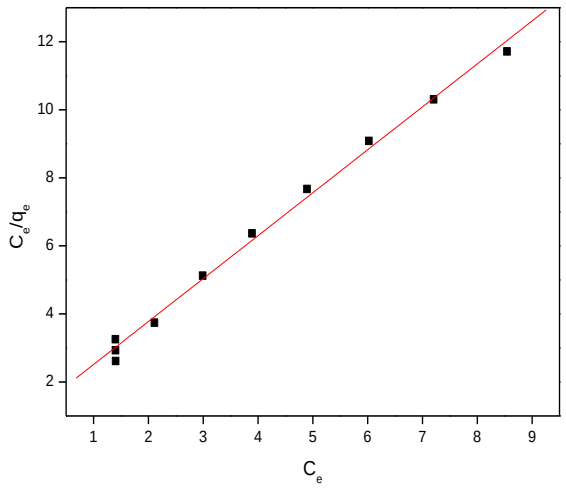


**Fig. 10. Langmuir adsorption isotherm for the adsorption of AB 10 by the $ZnFe_2O_4$-ZnO nanopowder**

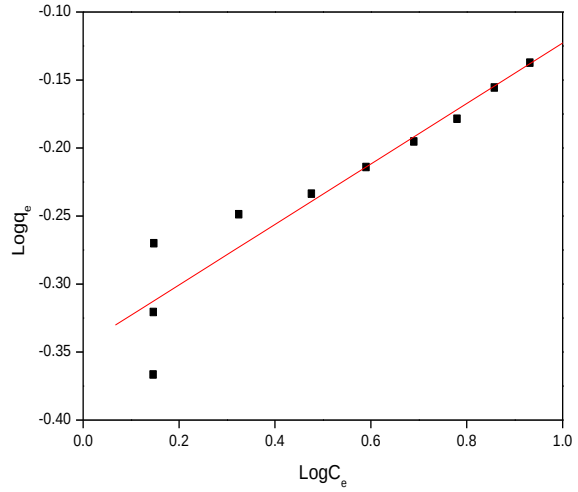


**Fig. 11. Freundlich adsorption isotherm for the adsorption of AB 10 by the ZnFe2O4-ZnO nanopowder**

**Table - I: Various isotherm parameters for the adsorption of AB 10 by the $ZnFe_2O_4$-ZnO nanopowder**

| Adsorption isotherm | Parameters | Value |
|---|---|---|
| Langmuir | $Q_0$ (mgg$^{-1}$) | 0.7921 |
| | b (Lmg$^{-1}$) | 1.0107 |
| | $R_L$ | 0.009 |
| | $R^2$ | 0.9946 |
| Freundlich | $K_F$ (mgg$^{-1}$) | 0.7081 |
| | n (gL$^{-1}$) | 4.4982 |
| | $R^2$ | 0.8845 |
| | E (kJmol$^{-1}$) | 2.3656 |

where, $q_e$ and $q_t$ indicate the amounts of dye adsorbed (mgg$^{-1}$) at equilibrium and at time *t* (min), respectively; and $k_1$ (min$^{-1}$) the rate constant of the pseudo-first order adsorption. The linear form of the Lagergren equation is given by using (9).

$$log\ (q_e - q_t) = log\ (q_e) - \frac{k_1 t}{2.303} \qquad (9)$$

The values of $k_1$ were calculated from the plots of $\log(q_e - q_t)$ versus *t*. The slope of the straight line is $-k_1/2.303$ and intercept $log(q_e)$.

The pseudo-second order equation based on the adsorption capacity can be expressed by using (10) [49]-[50].

$$\frac{dq_t}{dt} = k_2\ (q_e - q_t)^2 \qquad (10)$$

where $k_2$ (gmg$^{-1}$min$^{-1}$) is the rate constant of pseudo-second order adsorption.

Separating the variables in (10) gives (11).

$$\frac{dq_t}{(q_e - q_t)^2} = k_2 dt \qquad (11)$$

The linear form of the pseudo second order equation is represented by (12).

$$\frac{t}{q_t} = \frac{1}{k_2 {q_e}^2} + \frac{1}{q_e}\ t \qquad (12)$$

The values of $k_2$ and $q_e$ were calculated from the linear plot of $t/q_t$ versus *t*. The linear plot of $t/q_t$ versus *t* shows a good agreement of the experimental data with the pseudo-second order kinetic model. The good correlation coefficients for the pseudo-second order model justify the adsorption mechanism.

Fig. 12 and Fig. 13 represent the plots for the pseudo-first order and the pseudo-second order kinetic models. From Table II, it was evident that the $R^2$ value was higher in case of the pseudo-second order model compared to the pseudo-first order model. It was concluded that the adsorption of AB 10 by the $ZnFe_2O_4$-ZnO nanopowder followed pseudo-second order kinetic model.

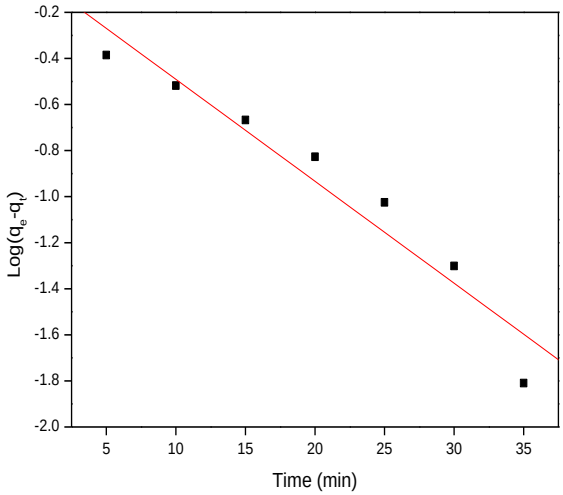


**Fig. 12. Pseudo-first order kinetic model for the adsorption of AB 10 by the $ZnFe_2O_4$-ZnO nanopowder**

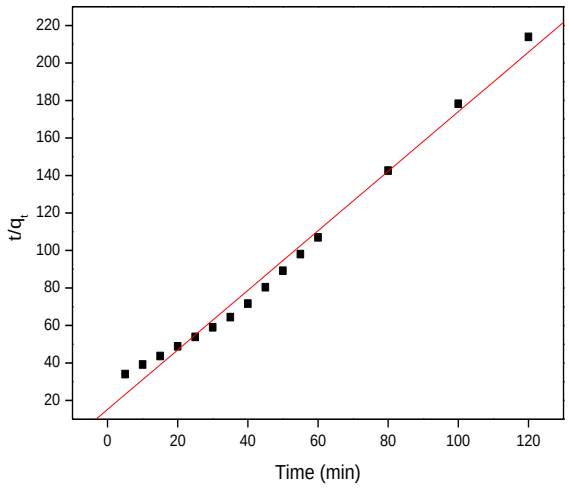


**Fig. 13. Pseudo-second order kinetic model for the adsorption of AB 10 by the ZnFe2O4-ZnO nanopowder**

**Table - II: Various kinetic parameters for the adsorption of AB 10 by the $ZnFe_2O_4$-ZnO nanopowder**

| Kinetic model | Parameters | Value |
|---|---|---|
| Pseudo-first order | $K_1$ ($min^{-1}$) | 0.1019 |
| | $R^2$ | 0.9351 |
| Pseudo-second order | $K_2$ ($gmg^{-1}min^{-1}$) | 0.1657 |
| | $R^2$ | 0.9872 |

## IV. CONCLUSION

$ZnFe_2O_4$-ZnO nanopowder was successfully prepared by solution combustion method and characterized by PXRD, FTIR, SEM and BET surface area techniques. The nanopowder was used as adsorbent for the removal of the dye Amido Black 10B from its aqueous solution. The effect of dosage of the nanopowder and contact time on the rate of adsorption was studied. The results indicated that the $ZnFe_2O_4$-ZnO nanopowder acted as a good adsorbent for the removal of AB 10. The adsorption was found to obey Langmuir adsorption isotherm and followed pseudo-second order kinetics. It was concluded that $ZnFe_2O_4$-ZnO nanopowder can be used as a good adsorbent material for the removal of dyes from textile and paper effluents.

## ACKNOWLEDGEMENT

The authors gratefully acknowledge the support rendered by the TEQIP Laboratory of M. S. Ramaiah Institute of Technology, Bengaluru, India for providing the facilities to carry out the research work.

## REFERENCES

1. S. Hegde, K. Nagaveni, and Sounak Roy, "Synthesis, structure and photocatalytic activity of nano TiO2 and nano TiMxO2-5 (M= Cu, Fe, Pt,Pd, V, W, Ce, Zr)," PRAMANA – Journal of Physics, vol. 65, 2005, pp. 641-645.
2. Saeedeh Hashemian, "MnFe2O4/bentonite nanocomposite as a novel magnetic material for adsorption of Acid Red 138," J. Biotech., vol. 9, 2010, pp. 8667-8671.
3. N. Madhusudhana, K. Yogendra, and K. Mahadevan, "Photocatalytic degradation of violet GL2B azo dye by using calcium aluminate nanoparticle in presence of solar light," Res. J. Chem. Sci., vol. 2, 2012, pp. 72-77.
4. A. Tuba, G. Tuğba, G. Afife, D. Gonul, and M. Ulku, "Decolourization of textile azo dyes by ultrasonication and microbial removal," Desalination, vol. 255, 2010, pp. 154-158.
5. K. Bubacz, J. Choina, D. Dolat, and A.W. Morawski, "Methylene blue and phenol photocatalytic degradation on nanoparticles of anatase TiO2," Polish J. of Environ. Stud., vol. 19, 2010, pp. 685-691.
6. E. N. Abrahart, "Dyes and their intermediates," New York Chemical Publishing, 1977, pp. 1-12.
7. M. Kucukosmanoglu, Orlon Gezici, and Ahmet Ayar, "The adsorption behaviors of methylene blue and methyl orange in a diaminoethane sporopollenin mediated column system," Purif. Technol., vol. 52, 2006, pp. 280-287.
8. W. Jiquan, W. Daojie, Z. Gaoke, g. Yadan, and L. Jin, "Adsorption of rhodamine B from aqueous solution onto heat activated sepiolite," Wuhan University Journal of Natural Sciences, vol. 18, 2013, pp. 219-225.
9. J. Huang, K. Huang, S. Liu, Q. Luo, and S. Shi, "Synthesis, characterization and adsorption behavior of aniline modified polystyrene resin for phenol in hexane and in aqueous solution," J. Coll. Interf. Sci., vol. 317, 2008, pp. 434-441.
10. S. A. Umoren, U. J. Etim, and A.U. Israel, "Adsorption of methyleneblue from industrial effluent using polyvinyl alcohol," J. Mater. Environ. Sci., vol. 4, 2013, pp. 75-86.
11. H. Ouasif, S. Yousfi, M.L. Bouamrani, M. El Kouali, S. Benmokhtar, and M. Talbi, "Removal of a cationic dye from wastewater by adsorption onto natural adsorbents," J. Mater. Environ. Sci., vol. 4, 2013, pp. 1-10.
12. H. Li, S. Gao, M. Cao, and R. Cao, "Self-assembly of polyoxometallate thionine multilayer films on magneticmicrospheres as photocatalyst for methyl orange degradation under visible light irradiation," J. Coll. Interf. Sci., vol. 394, 2013, pp. 434-440.
13. V.K. Garg, "Removal of a basic dye from aqueous solution by adsorption using timber industry waste," Chem. Biochem. Eng., vol. 19, 2005, pp. 75-80.
14. D. Kavitha, and C. Namasivayam, "Experimental and kinetic studies on methylene blue adsorption by coir pith carbon," Bioresour. Technol., vol. 98, 2007, pp. 14-21.
15. A. Khenifi, "Adsorption study of an industrial dye by an organic clay," Adsorption, vol. 13, 2007, pp. 149-158.
16. Sina Saremi-Yarahmadi, Asif Ali Tahir, B. Vaidhyanathan, and K. G. U. Wijayantha, "Fabrication of nanostructured α-Fe2O3 electrodes using ferrocene for solar hydrogen generation," Mater. Lett., vol. 63, 2009, pp. 523-526.
17. L. Y. Novoselova, "Structure and properties of composite nanomaterials: products of the thermal treatment of molybdenum and iron containing powders," Russ. J. Phys. Chem. A, vol. 86, 2012, pp. 1689–1696.
18. Abhipsa Mahapatra, "Fabrication and characterization of novel iron oxide/ alumina nanomaterials for environmental applications," Ph.D., Thesis, 2013, pp. 4.
19. Abdul Hameed, Valentina Gombac, Tiziano Montini, Mauro Graziani, and Paolo Fornasiero, "Synthesis, characterization and photocatalytic activity of NiO-Bi2O3 nanocomposites," Chem. Phys. Lett., vol. 472, 2009, pp. 212-216.
20. C. Hu, T. Lu, F. Chen, and R. Zhang, "A brief review of graphene-metal oxide composites synthesis and applications in photocatalysis," J. Chinese Adv. Mater. Soc., vol. 1, 2013, pp. 21-39.
21. L. P. Balet, S. A. Ivanov, A. Piryatinski, M. Achermann, and V. I. Klimov, "Inverted core/shell nanocrystals continuously tunable between Type I and Type II localization regimes," Nano Lett., vol. 4, 2004, pp. 1485-1488.
22. Ambreen Lateef, and Rabia Nazir, "Metal Nanocomposites: Synthesis, Characterization and their Applications, Science and Applications of Tailored Nanostructures," One Central Press, 2013, Chapter 12, pp. 239-256.
23. M. N. Zulfiqar Ahmed, K. B. Chandrasekhar, A. A. Jahagirdar, H. Nagabhushana, and B. M. Nagabhushana, "Photocatalytic activity of nanocrystalline ZnO, α-Fe2O3 and ZnFe2O4/ZnO," Appl. Nanosci., vol. 5, 2015, pp. 961–968.
24. M. N. Zulfiqar Ahmed, K. B. Chandrasekhar, A. A. Jahagirdar, H. Nagabhushana, and B. M. Nagabhushana, "Synergistic mechanism of ZnFe2O4/ZnO nanopowder in photocatalytic degradation of Acid Orange 7," Asian Journal of Chemistry, vol. 3, 2018, pp. 607–612.
25. A. A. Jahagirdar, M. N. Zulfiqar Ahmed, N. Donappa, H. Nagabhushana, and B. M. Nagabhushana, "Synthesis, characterization and dye degradation activity of α-Fe2O3," IJETA-ETS, vol. 4, 2011, pp. 144-147.

26. K. C. Patil, M. S. Hegde, Tanu Rattan and S. T. Aruna, "Chemistry of Nanocrystalline Oxide Materials: Combustion Synthesis, Properties and Applications," World Scientific Publishing Co. Pvt. Ltd., Singapore, 2008, pp. 332.
27. P. Muthirulan, C. N. Devi, and M. M. Sundaram, "A green approach to the fabrication of titania-graphene nanocomposites: insights relevant to efficient photodegradation of Acid Orange 7 dye under solar irradiation," Mat. Sci. Semicond. Process, vol. 25, 2014, pp. 219-230.
28. http://www.chemicalland21.com/specialtychem/finechem/AMIDO%20 BLACK %2010B.htm, accessed on September 15, 2012.
29. https://www.alfa.com/en/catalog/A11374/, accessed on September 15, 2012.
30. Marjan Tanzifi, Mohsen Mansouri, Maryam Heidarzadeh, and Kobra Gheibi, "Study of adsorption of Amido Black 10B dye from aqueous solution using polyaniline nano-adsorbent: Kinetic and isotherm studies," J. Water Environ. Nanotechnol., vol. 1, 2016, pp. 124-134.
31. 31. http://www.bio-rad.com/webroot/web/pdf/WWMSDS/LSGC/USA /USA_USA_1610402.pdf, accessed on September 15, 2012.
32. Loghman Karimi, Salar Zohoori, and Mohammad Esmail Yazdanshenas, "Photocatalytic degradation of azo dyes in aqueous solutions under UV irradiation using nano-strontium titanate as the nanophotocatalyst," J. Saudi Chem. Soc., vol. 18, 2014, pp. 581-588.
33. M. Mehrabian, R. Azimirad, K. Mirabbaszadeh, H. Afarideh, and M. Davoudian, "UV detecting properties of hydrothermal synthesized ZnO nanorods," Physica E: Low-dimensional Systems and Nanostructures, vol. 43, 2011, pp. 1141-1145.
34. C. Klingshirn, "ZnO: Material, Physics and Applications," Chemphyschem: A European Journal of Chemical Physics and Physical Chemistry, vol. 8, 2007, pp. 782-803.
35. Yun Li, Guozhang Dai, Chunjiao Zhou, Qinglin Zhang, Qiang Wan, Limin Fu,; Jianping Zhang, Ruibin Liu, Chuanbao Cao, Anlian Pan, Yunhong Zhang, and Bingsuo Zou, "Formation and optical properties of ZnO:ZnFe2O4 superlattice microwires," Nano Res., vol. 3, 2010, pp. 326-338.
36. A. Azadeh, A. Mohammad Amin, and Ali Morsali, "Sonochemically assisted synthesis of ZnO nanoparticles: A novel direct method, Iran. J. Chem. Chem. Eng., vol. 30, 2011, pp. 75-81.
37. Thomas Marykutty, and K. C. George, "Infrared and magnetic study of nanophase zinc ferrite," Ind. J. Pure Appl. Phys., vol. 47, 2009, pp. 81-86.
38. B. P. Ladgaonkar, C. B. Kolekar, and A. S. Vaingankar, "Infrared absorption spectroscopic study of Nd+3 substituted Zn-Mg ferrites," Bull. Mater. Sci., vol. 25, 2002, pp. 351-354.
39. S. Sumetha, "Structural and optical properties of nanocrystalline ZnO powder from sol-gel method," Sci. Asia, vol. 34, 2008, pp. 31-34.
40. 40. E. Darezereshki, "One-step synthesis of hematite (α-Fe2O3) nanoparticles by direct thermal-decomposition of maghemite," Mater. Lett., vol. 65, 2011, pp. 642-645.
41. I. Wayan Sutapa, Abdul Wahid Wahab, Paulina Taba, and Nursiah La Nafie, "Synthesis and structural profile analysis of the MgO nanoparticles produced through the sol-gel method followed by annealing process," Orient. J. Chem., vol. 34, 2018, pp. 1016-1025.
42. M. N. Zulfiqar Ahmed, K. B. Chandrasekhar, A. A. Jahagirdar, H. Nagabhushana, and B. M. Nagabhushana, "Photocatalytic activity of nanocrystalline ZnO, α-Fe2O3 and ZnFe2O4/ZnO," Appl. Nanosci., vol. 5, 2015, pp. 961-968.
43. N. M. Deraz, and A. Alarifi, "Microstructure and magnetic studies of zinc ferrite nano-particles," Int. J. Electrochem. Sci., vol. 7, 2012, pp. 6501-6511.
44. K. Vijayaraghavan, T. V. N. Padmesh, K. Palanivelu, and M. Velan, "Biosorption of nickel(II) ions onto Sargassum wightii: Application of two-parameter and three-parameter isotherm models," J. Hazard. Mater. B, vol. 133, 2006, pp. 304-308.
45. G. McKay, H. S. Blair, and J. Gardner, "The adsorption of dyes on chitin III, Intraparticle diffusion processes," J. Appl. Polym. Sci., vol. 28, 1983, pp. 1767-1778.
46. Mohammed Ahmaruzzaman, "Adsorption of phenolic compounds on low-cost adsorbents: A review," Adv. Colloid. Interface Sci., vol. 143, 2008, pp. 48-67.
47. A. Gunay, E. Arslankaya, and I. Tosun, "Lead removal from aqueous solution by natural and pretreated clinoptilolite: adsorption equilibrium and kinetics," J. Hazard. Mater., vol. 146, 2007, pp. 362-371.
48. G. McKay, and Y. S. Ho, "The sorption of lead(ii) on peat," Water Res., vol. 33, 1999, pp. 578-584.
49. Hiu QIU, L.V. LV, Bing-cai PAN, Qing-jian ZHANG, Wei-ming ZHANG, and Quan-xing ZHANG, "Critical review in adsorption kinetic models," Journal of Zhejiang University-SCIENCE A, vol. 10, 2009, pp. 716-724.
50. B. H. Hameed, D. K. Mahmoud, and A. L. Ahmad, "Equilibrium modeling and kinetic studies on the adsorption of basic dye by a low-cost adsorbent: coconut (Cocos nucifera) bunch waste," J. Hazard. Mater., vol. 158, 2008, pp. 65-72.

## AUTHORS PROFILE

**M. N. Zulfiqar Ahmed** completed his M.Sc. in Chemistry from Bangalore University and is pursuing his doctoral degree in chemistry from Jawahrlal Nehru Technological University Anatapur, Andhra Pradesh. He is currently working as Faculty of Chemistry, Department of Engineering, Ibri College of Technology, Ibri, Sultanate of Oman. He has co-authored a book on nano metal oxides and published a few papers in the field of nanotechnology.

**Dr. A. A. Jahagirdar** completed his M.Sc. in Chemistry from Karnataka University. He completed his Ph.D. in Chemistry and has participated in several national and international conferences. He has authored a book on nano metal oxides and has published several research papers on nanomaterials in international journals. He is a member of several professional bodies. He is currently working as Professor in the Department of Chemistry, Dr. Ambedkar Institute of Technology, Bengaluru, India.

**Dr. H. M. Somashekar** completed his M. Tech .in Engineering Management from Visvesvaraya Technological University and Ph.D. in Mechanical Engineering from Bangalore University. He has guided a number of students at the Bachelor and Masters Level. He is also a guide for several Ph.D. students. He has published several research papers in international journals and also participated in a number of workshops, national and international conferences. He is currently working as Assistant professor in the Department of Mechanical Engineering, Dr. Ambedkar Institute of Technology, Bengaluru, India.